American Mineralogist, Volume 69, pages 399–403, 1984

Extinction angles for monoclinic amphiboles or pyroxenes: a cautionary note

SHU-CHUN SU[1,2] AND F. D. BLOSS[1]

Department of Geology, University of New Mexico
Albuquerque, New Mexico 87131

Abstract

For monoclinic crystals with **b** = Y, extinction angles measured relative to a {110} cleavage trace will equal the optic orientation angle $Z \wedge$ **c** (or $X \wedge$ **c**) only for (010) sections. Such sections are best recognized from display of a centered optic normal figure and, as long known, are not necessarily the section in the [001] zone that exhibits the maximum extinction angle relative to the {110} cleavage trace. Such maximum extinction angles are here proved to exceed $Z \wedge$ **c** (or $X \wedge$ **c**) for optic orientations where **b** = Y, if the obtuse bisectrix is within 45° of **c**. Indeed, if **c** also happens to lie in or near a circular section of the optical indicatrix, maximum extinction angles for sections in the [001] zone may approach 45° regardless of the value of $Z \wedge$ **c** (or $X \wedge$ **c**). A hornblende from Mt. Monadnock, New Hampshire—for which Winchell and Winchell (1951) cite $2V_z$ = 137° and $Z \wedge$ **c** = 21°—closely approaches this special case because its angles V_z and $Z \wedge$ **c** are almost complementary.

Introduction

For monoclinic amphiboles and pyroxenes in thin sections, the maximum extinction angle, if measured from grains oriented so that their {110} cleavage appears as a single set of mutually parallel traces, is usually assumed to have been measured from a (010) section and thus to represent the angle $Z \wedge$ **c** (or $X \wedge$ **c**). Frequently forgotten are the cautions of long ago (Daly, 1899; Duparc and Pearce, 1907; Rosenbusch and Wülfing, 1921–24) and of recent times (Hartshorne and Stuart, 1970). These note that, for crystal sections parallel to *c*, the maximum extinction angle relative to {110} cleavage traces may occur for sections *at a significant angle* ϕ *to* (010) and, in such case, may significantly exceed $Z \wedge$ **c** (or $X \wedge$ **c**). In the appendix, we prove that this will occur for monoclinic crystals with {*hk*0} cleavage and **b** = Y only if the obtuse bisectrix lies within 45° of **c**. Such orientations occur for several common amphiboles and pyroxenes. Table 1, to be discussed next, permits petrographers to estimate the degree to which the maximum extinction angle will exceed the optic orientation angle $Z \wedge$ **c** (or $X \wedge$ **c**) if measured from sections parallel to **c** at varying angles ϕ relative to (010).

Discussion

In Table 1 the column heads—namely, 5, 10 . . . to, at most, 40—represent the angle (in degrees) between the obtuse bisectrix (*0B*) and the **c** axis. The vertical column at left represents ϕ, the dihedral angle between (010) and the crystal section parallel to **c** from which the extinction angle E was measured relative to the {*hk*0} cleavage traces. Values in the body of the Table 1 represent E for different combinations of the obtuse optic angle $2V_{0B}$, ϕ, and *0B* $\wedge$ **c**.

Vertical columns headed by those values of *0B* $\wedge$ *c* which are complements of V_{0B} represent special orientations where **b** = Y *and* where the **c** axis lies within a circular section of the optical indicatrix. For these columns wherein

$$(0B \wedge c) + V_{0B} = 90° \qquad (1)$$

the angle E, regardless of the value of *0B* $\wedge$ **c**, approaches 45° as ϕ approaches 90°. For ϕ precisely equal to 90°, the section will lie parallel to (100). In such a case, to the extent that Equation (1) holds for the crystal, this section will be perpendicular to an optic axis and thus will have no well defined extinction position. However, a plane at a small angle δ to (100) *will* have a defined extinction angle (Fig. 1). As shown, the two circular sections intersect this particular plane at the two black dots. Following the Biot–Fresnel rule, the hollow point v, which bisects the angle between the two black dots, represents the privileged direction for the dashed plane. Note that this privileged direction is almost at 45° to the **c** axis, and thus to the trace of the {110} cleavage on this dashed plane.

For a crystal that exactly conforms to Equation (1), a plot of E versus ϕ discloses (Fig. 2A) that the true angle *0B* $\wedge$ **c** corresponds to the *minimum* value for E, not the

[1] Present address: Department of Geological Sciences, Virginia Polytechnic Institute and State University, Blacksburg, Virginia 24061.

[2] Permanent address: Institute of Geology, Chinese Academy of Sciences, Beijing, The People's Republic of China.

0003–004X/84/0304–0399$02.00

Table 1. Extinction angles relative to {*hk*0} cleavage for (*hk*0) planes at varying interfacial angles ϕ to (010) and for different optic orientations **c**:0B and 2*V* angles*

ϕ = (010) ∧ SECTION IN PRISM ZONE

ϕ	2V = 100°								2V = 170°
0*	**5.0**	**10.0**	**15.0**	**20.0**	**25.0**	**30.0**	**35.0**	**40.0**	**5.0**
10	5.0	10.0	15.0	20.0	25.1	30.1	35.1	40.1	5.1
20	5.0	10.1	15.1	20.2	25.2	30.2	35.3	40.3	5.3
30	5.1	10.2	15.2	20.3	25.4	30.5	35.6	40.7	5.8
40	5.1	10.1	15.2	20.4	25.5	30.7	35.9	41.2	6.5
50	4.9	9.9	14.9	20.1	25.3	30.7	36.2	41.8	7.7
60	4.5	9.1	13.9	18.9	24.3	30.1	36.2	42.5	9.7
70	3.6	7.3	11.4	16.0	21.4	27.8	35.2	43.3	13.6
80	2.0	4.2	6.7	9.9	14.2	20.5	30.3	44.1**	22.7**
90	0.0	0.0	0.0	0.0	0.0	0.0	0.0	45.0	45.0

ϕ	2V = 110°							2V = 160°	
0*	**5.0**	**10.0**	**15.0**	**20.0**	**25.0**	**30.0**	**35.0**	**5.0**	**10.0**
10	5.0	10.1	15.1	20.1	25.1	30.1	35.1	5.1	10.1
20	5.1	10.2	15.3	20.4	25.4	30.5	35.6	5.3	10.6
30	5.2	10.4	15.6	20.8	26.0	31.1	36.3	5.7	11.4
40	5.3	10.6	15.9	21.3	26.6	31.9	37.2	6.4	12.7
50	5.3	10.7	16.1	21.6	27.1	32.8	38.4	7.4	14.8
60	5.1	10.2	15.6	21.3	27.2	33.5	39.8	9.1	18.0
70	4.2	8.7	13.6	19.2	25.8	33.3	41.5	11.9	23.4
80	2.5	5.3	8.6	13.0	19.4	29.3	43.2	15.2	32.2**
90	0.0	0.0	0.0	0.0	0.0	0.0	45.0**	0.0	45.0

ϕ	2V = 120°						2V = 150°		
0*	**5.0**	**10.0**	**15.0**	**20.0**	**25.0**	**30.0**	**5.0**	**10.0**	**15.0**
10	5.0	10.1	15.1	20.1	25.2	30.2	5.1	10.1	15.2
20	5.1	10.3	15.4	20.6	25.7	30.8	5.3	10.5	15.8
30	5.3	10.6	16.0	21.2	26.5	31.7	5.6	11.3	16.8
40	5.5	11.1	16.6	22.2	27.6	33.1	6.2	12.4	18.5
50	5.7	11.5	17.3	23.2	29.0	34.8	7.1	14.1	21.0
60	5.7	11.6	17.6	23.9	30.4	36.9	8.3	16.5	24.6
70	5.1	10.5	16.5	23.4	31.1	39.4	9.8	19.7	29.7
80	3.2	6.9	11.5	18.1	28.2	42.1**	9.5	21.4	36.6**
90	0.0	0.0	0.0	0.0	0.0	45.0	0.0	0.0	45.0

ϕ	2V = 130°					2V = 140°			
0*	**5.0**	**10.0**	**15.0**	**20.0**	**25.0**	**5.0**	**10.0**	**15.0**	**20.0**
10	5.0	10.1	15.1	20.2	25.2	5.1	10.1	15.2	20.2
20	5.2	10.4	15.6	20.7	25.9	5.2	10.5	15.7	20.9
30	5.4	10.9	16.3	21.7	27.0	5.6	11.1	16.6	22.0
40	5.8	11.6	17.3	23.0	28.6	6.0	12.0	18.0	23.8
50	6.2	12.4	18.6	24.8	30.8	6.7	13.3	19.8	26.3
60	6.5	13.1	19.9	26.8	33.6	7.4	14.8	22.3	29.6
70	6.3	12.9	20.3	28.4	37.0	7.8	16.0	24.8	33.9
80	4.4	9.5	16.4	26.7	40.9**	6.3	13.9	24.7	39.2**
90	0.0	0.0	0.0	0.0	45.0	0.0	0.0	0.0	45.0

* The extinction angles for phi equal 0°, here designated with slightly bolder type, precisely equal the c:OB angle which the petrographer seeks. The columns headed with a bold 5.0° thus show how extinctions observed for an (*hk*0) plane vary as their phi angle relative to (010) in turn varies from 0°, 10° . . . to 90°.

** These extinction angles closely approach 45° and are for phi angles slightly less than 90°. If phi exactly equals 90°, this extinction angle becomes indeterminate.

maximum. This holds true if we exclude from consideration sections for which ϕ nearly or exactly equals 90° Fortunately, such sections are readily recognized (low birefringence and near-centered optic axis figures). By contrast the desired sections, at or near ϕ equal 0°, will display a centered optic normal figure (and thus maximum retardation). However, even if ϕ equals as much as 20° (*cf.* Table 1), the measured *E* angles will exceed *0B* ∧ **c** by only 6% at most.

The data of Winchell and Winchell (1951) for a hornblende from Mt. Monadnock, New Hampshire—$2V_Z$ = 137° and *Z* ∧ **c** = 20–21°—provide a practical example.

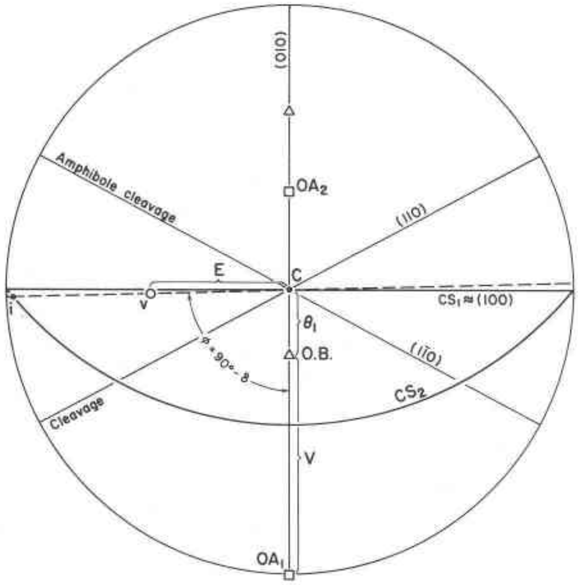

Fig. 1. Stereographic projection of a monoclinic hornblende crystal from Mt. Monadnock, New Hampshire, using the data—$Z \wedge \mathbf{c} = 21°$; $2V_X = 43°$—given by Winchell and Winchell (1951, p. 435). For this crystal, the **c** axis lies practically within a circular section of the indicatrix because

$$Z \wedge \mathbf{c} + V_Z \approx 89.5°$$

The dashed line represents a plane parallel to **c** which lies at an angle ϕ, namely $90° - \delta$ where δ is extremely small, to the optic plane (010). This dashed line intersects one circular section (CS_1) at **c** and the other (CS_2) at *i*. Consequently *v*, the vibration direction for light normally incident on the plane represented by this dashed line, is the bisector of the angle between **c** and *i*. Point *c* also represents the intersection between said plane and any {*hk*0} cleavage. Accordingly, *E* equals the extinction angle for light normally incident on said plane if measured relative to an {*hk*0} cleavage trace. For this special case, note that extinction angle *E* has approached 45° even though $Z \wedge \mathbf{c}$ only equals 21°.

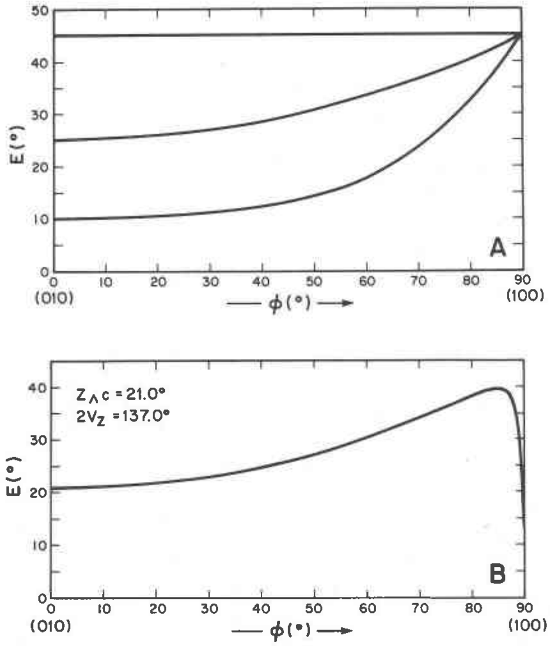

Fig. 2(A). Values of the extinction angles relative to {*hk*0} cleavage for a family of planes parallel to **c** as their interfacial angle (ϕ) relative to (010) varies from 0° to 90°. The three curves represent three different crystals for which, respectively, the angle between the obtuse bisectrix and **c** equals 10°, 25° and 45°. Each crystal has an obtuse angle *V*, which is the complement of its $\mathbf{c} \wedge OB$ angle. In such case the plane for which ϕ equals 90°—that is, the (100) plane—coincides with a circular section of the indicatrix and, accordingly, lacks a specific privileged direction so that the extinction angle *E* is not defined for this orientation. Contrary to common belief, the angle $\mathbf{c} \wedge OB$ would represent the minimum extinction angle measured in this section for these special cases. The top curve represents a correction of the top curve in Fig. 7.24 of Hartshorne and Stuart (1970). (B) Plot of *E* versus ϕ for the hornblende from Mt. Monadnock, New Hampshire.

Accepting $Z \wedge \mathbf{c}$ as 21°, our calculations of *E* versus ϕ, if plotted (Fig. 2B), disclose that *E* drops off preciоitously to 0°, as ϕ exceeds (*ca.*) 85°.

Amphibole crystals in oil (or Canada balsam) mounts likely lie on a {110} cleavage. If so, this plane of rest will be at an angle ϕ of (*ca.*) 62° to the (010) plane. For amphiboles with $\mathbf{b} = Y$ and with **c** within 45° of the obtuse bisectrix, the extinction angles measured from such mounted grains will thus exceed $Z \wedge \mathbf{c}$ (or $X \wedge \mathbf{c}$). Comparing the *E* angles for $\phi \approx 60°$ to those for $\phi = 0°$ in Table 1 indicates the extent of the expected discrepancy. Similarly, for grain mounts of pyroxenes, the values for $\phi = 45°$ should be compared to the values obtained by interpolating halfway between those at $\phi = 40°$ and $\phi = 50°$ in Table 1.

Acknowledgments

This work was supported by the Caswell Silver Foundation during our stimulating stay in the University of New Mexico Department of Geology. We thank Dr. Ray E. Wilcox and Professor Max Carman for their helpful reviews of the original manuscript. Support from the National Science Foundation (NSF EAR-8018492) is also gratefully acknowledged.

References

Bloss, F. D. (1981) The Spindle Stage. Principles and Practice. Cambridge University Press, New York.

Daly, R. A. (1899) On the optical characters of the vertical zone of amphiboles and pyroxenes; and on a new method of determining the extinction angles of these minerals by means of cleavage pieces. Proceedings of the American Academy of Arts and Sciences. 34, 311–323.

Duparc, L. and Pearce, F. (1907) Traité de technique minéralogique et pétrographique, I. Leipzig.

Hartshorne, N. H. and Stuart, A. (1970) Crystals and the Polarising Microscope. Fourth edition, Elsevier, New York.

Rosenbusch, H. and Wülfing, E. A. (1921/1924) Mikroscopische Physiographie, Vol. 1, Part 1, Stuttgart.

Winchell, A. N. and Winchell, H. (1951) Elements of Optical Mineralogy. Fourth edition. Part II. Descriptions of Minerals. John Wiley and Sons, New York.

Wright, F. E. (1923) The formation of interference figures. Journal of Optical Society of America and Review of Scientific Instruments. 7, 779–817.

Manuscript received, August 23, 1982;
accepted for publication, August 30, 1983.

Appendix

Previously we stated without proof that, for monoclinic crystals with {*hk*0} cleavage and **b** = *Y*, the extinction angle *E* can exceed $Z \wedge c$ (or $X \wedge c$) only if the obtuse bisectrix is at less than 45° to the **c** axis. To prove this, let **c** and *Z* (Fig. 3A) represent the **c** axis and one bisectrix of the optical indicatrix for a monoclinic crystal with **b** = *Y* and {*hk*0} cleavage. The bold ellipse represents an equivibration curve (Wright, 1923, p. 785; Bloss, 1981, p. 100–106) which by definition represents the locus of all points that represent radii of equal length within this crystal's optical indicatrix. The dashed line represents the direct projection of a plane, in the [001] zone, at a random angle ϕ to the (010) plane. This dashed plane intersects the equivibration curve at **c** and *P*. Because **c** and *P* are radii of equal length in the indicatrix, the hollow dot representing the line that bisects the angle between **c** and *P* is necessarily a privileged direction for light normally incident on this dashed plane. By varying ϕ between 0° and 90°, the dashed plane can represent the entire family of planes parallel to [001]. Note that, for any plane in this family, the angle $\mathbf{c} \wedge P$ equals twice the extinction angle *E* as measured relative to the {*hk*0} cleavage for light normally incident on the dashed plane.

In Figure 3A, θ_1, θ_2 and θ_3 respectively represent angles $\mathbf{c} \wedge Z$, $P \wedge Z$, and $P_0 \wedge X$—where P_0 represents the intersection between the indicatrix's *XY* plane and the plane containing *P* and *Z*. Each pair of lines—**c** and *Z*, *P* and *Z*, P_0 and *X*—defines a plane which intersects the indicatrix in an ellipse (Figs 3B, 3C and 3D). Hence, from the equation for an ellipse, the lengths of radii of the indicatrix corresponding to **c**, P_0 and *P* can be written

$$c^{-2} = \gamma^{-2} \cos^2\theta_1 + \alpha^{-2} \sin^2\theta_1 \tag{2}$$

$$P_0^{-2} = \alpha^{-2} \cos^2\theta_3 + \beta^{-2} \sin^2\theta_3 \tag{3}$$

$$P^{-2} = \gamma^{-2} \cos^2\theta_2 + P_0^{-2} \sin^2\theta_2 \tag{4}$$

The right hand side (r.h.s.) for Equation 3 can substitute for P_0^{-2} in Equation 4 and, since radii *c* and *P* are equal (because both plot on the same equivibration curve), the *r.h.s.* of Equations 2 and 4 may be equated. Dividing the resultant equation by $(\alpha^{-2} - \gamma^{-2})$ and then substituting $\sin^2V_Z$ for $(\alpha^{-2} - \beta^{-2})/(\alpha^{-2} - \gamma^{-2})$, we obtain

$$\sin^2\theta_2 = \frac{\sin^2\theta_1}{1 - \sin^2\theta_3 \sin^2V_Z} \tag{5}$$

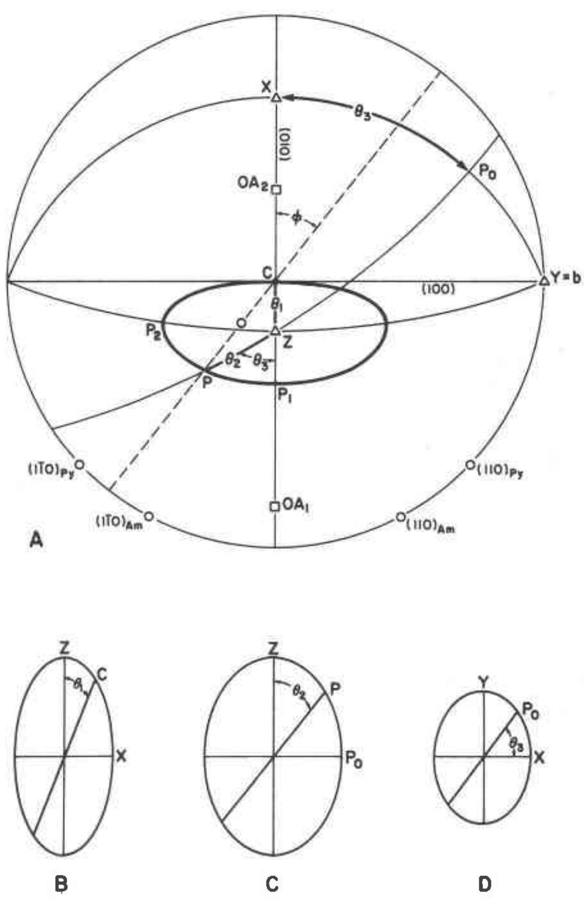

Fig. 3(A). Stereographic projection of a crystal for which Z : **c** equals 21° and $2V_Z$ = 118°. The ellipse (bold line) represents an equivibration curve representing the loci of all radii in the crystal's optical indicatrix whose lengths equal a particular value of γ': The dashed line through *c* represents the direct projection of one of the family of planes parallel to **c** which is at an angle ϕ relative to (010). This plane intersects the equivibration curve at **c** and at *P*. The plane containing *P* and *Z* has been extended until it intersects the indicatrix's *XY* plane at P_0. The angles θ_1, θ_2, and θ_3 are thus defined as $\mathbf{c} \wedge Z$, $P \wedge Z$, and $P_0 \wedge X$, respectively. (B) Cross-section through the optical indicatrix for the plane containing *Z* and **c**; (C) One for that containing *Z* and *P*; and (D) One for that containing *X* and *Y*. Angles θ_1, θ_2, and θ_3 are as illustrated.

or

$$\cos^2\theta_2 = \frac{\cos^2\theta_1 - \sin^2\theta_3 \sin^2V_Z}{1 - \sin^2\theta_3 \sin^2V_Z} \tag{6}$$

Our proof is simplified, but not negated, if we equate θ_3 to 90° so that equation 6 becomes

$$\cos^2\theta_2 = \frac{\cos^2\theta_1 - \sin^2V_Z}{\cos^2V_Z} \tag{7}$$

For θ_3 equal 90°, point P moves to position P_2 (Fig. 3A) and from the spherical right triangle cZP_2,

$$\cos 2E = \cos \theta_1 \cos \theta_2 \tag{8}$$

where $2E$ represents twice the extinction angle for the plane containing radii c and P_2. If E is to exceed θ_1, then necessarily

$$\cos 2\theta_1 > \cos 2E$$

and, in consequence of this and equation 8,

$$\cos^2 2\theta_1 > \cos^2\theta_1 \cos^2\theta_2 \tag{9}$$

Table 2 summarizes the algebraic manipulations whereby, as a consequence of inequality (9), we show that

$$\tan^2 \theta_1 + \tan^2 V_Z > 2 \tag{10}$$

The angle θ_1, equal to $Z \wedge c$ in our example, by convention is less than 45°. Accordingly, for inequality (10) to hold, V_Z must exceed 45°. In other words, extinction angle E can exceed θ_1, if $\theta_3 = 90°$, only if the indicatrix bisectrix closest to c is the obtuse bisectrix.

Table 2. Algebraic steps that lead from Equation 9 to Equation 10 in the text

$\cos^2 2\theta_1 > \cos^2\theta_1 \cdot \cos^2\theta_2$	Eq 9
$4\cos^4\theta_1 - 4\cos^2\theta_1 + 1 > \cos^2\theta_1 \cos^{-2}V_Z(\cos^2\theta_1 - \sin^2V_Z)$	
$\cos^2V_Z - 4\cos^2\theta_1 \sin^2\theta_1 \cos^2V_Z > \cos^4\theta_1 - \cos^2\theta_1 \sin^2V_Z$	
$\cos^2V_Z - \cos^2\theta_1(1-\sin^2\theta_1) + \cos^2\theta_1\sin^2V_Z - 4\cos^2\theta_1\cos^2V_Z\sin^2\theta_1 > 0$	
$\cos^2V_Z + \cos^2\theta_1\sin^2\theta_1 - \cos^2\theta_1\cos^2V_Z - 4\cos^2\theta_1\cos^2V_Z\sin^2\theta_1 > 0$	
$\cos^2V_Z\sin^2\theta_1 + \cos^2\theta_1\sin^2\theta_1 - 4\cos^2\theta_1\cos^2V_Z\sin^2\theta_1 > 0$	
$\sin^2\theta_1 > 0$, $\cos^2\theta_1 > 0$ and $\cos^2V_Z > 0$, we have	
$\cos^{-2}\theta_1 + \cos^{-2}V_Z > 4$	
or $\tan^2\theta_1 + \tan^2V_Z > 2$	Eq 10